Society of Medical Education & Research

2025, Volume 5, Issue 2, Page No: 159-172
ISSN: 3108-4834

Archive of International Journal of Cancer and Allied Science

# Mitochondrial Glutamine Metabolism Modulates Chemotherapy Sensitivity in Cancer Cells through Amphiregulin Signaling

**Filip Adam Novak[1]*, Jan Martin Hruby[1], Petra Eva Kolar[1]**

[1]Department of Oncology, Charles University Faculty of Medicine, Prague, Czech Republic.

***E-mail** ✉ f.novak.cuni@yahoo.com

## Abstract

Genomic stability relies on an effective DNA damage response (DDR), which serves as a critical barrier against tumor development. Yet, how cellular metabolism adapts to DNA damage remains largely unexplored, limiting opportunities to develop metabolism-targeted cancer therapies [Ref]. Emerging evidence suggests that DDR is closely linked to metabolic control, particularly through the restriction of glutamine (Gln) import into mitochondria, a process that supports both cell cycle arrest and DNA repair [Ref]. In this work, we identify mitochondrial Gln metabolism as a key determinant of cell fate following DNA damage. Specifically, inhibition of glutaminase (GLS)—the enzyme responsible for initiating Gln-driven anaplerosis—renders cancer cells more susceptible to DNA damage by triggering the expression of amphiregulin (AREG), which drives apoptotic cell death. Mechanistically, GLS suppression elevates reactive oxygen species (ROS), which in turn activates AREG transcription via the Max-like protein X (MLX) transcription factor. Notably, disrupting mitochondrial Gln metabolism markedly enhances chemotherapy-induced cell death in both cell culture and animal models. Together, these findings reveal a previously unrecognized role of mitochondrial Gln metabolism in DDR-induced apoptosis and point to novel metabolic strategies for improving cancer therapy.

**Keywords:** Mitochondrial, glutamine (Gln), Chemotherapy, Amphiregulin

## Introduction

Cells constantly face a variety of endogenous and exogenous insults that damage DNA. To maintain genomic integrity, they rely on a sophisticated DNA damage response (DDR) network that coordinates growth arrest, DNA repair, and, when necessary, programmed cell death. Disruptions in these tightly regulated pathways are a major source of genomic instability and contribute to human diseases such as cancer and aging [1-3]. Increasing evidence highlights the critical role of cellular metabolism in shaping adaptive responses to DNA damage and influencing whether a cell survives, arrests, or dies under genotoxic stress [2, 4]. Identifying the metabolic pathways that respond to DNA damage could thus provide key insights into the link between metabolism and DDR and inform strategies for cancer prevention or therapy.

Glutamine (Gln), the most abundant amino acid in the body, is a central carbon source for the mitochondrial tricarboxylic acid (TCA) cycle [5]. Its metabolism is crucial for balancing cell proliferation and growth arrest. Highly proliferative cells, including many cancer types, rely heavily on mitochondrial Gln metabolism to generate TCA-derived precursors for nucleotides, lipids, and proteins [6 ,7], which explains their metabolic dependence on Gln [8]. Our previous work also demonstrated that mitochondrial Gln metabolism regulates cellular senescence [9]. Interestingly, genotoxic stress suppresses mitochondrial Gln metabolism by limiting the entry of Gln into the TCA cycle, a mechanism required for proper cell cycle arrest and efficient DNA repair. Disruption of this metabolic

**Access this article online** https://smerpub.com/

**Received:** 09 August 2025; **Accepted:** 28 November 2025



**How to cite this article:** Novak FA, Hruby JM, Kolar PE. Mitochondrial Glutamine Metabolism Modulates Chemotherapy Sensitivity in Cancer Cells through Amphiregulin Signaling. Arch Int J Cancer Allied Sci. 2025;5(2):159-72. https://doi.org/10.51847/2BrxGEYG9g

checkpoint leads to defective DDR and delayed repair processes [10]. These observations suggest that mitochondrial Gln metabolism may play an underappreciated role in determining cell survival following DNA damage, but its involvement in apoptosis remains largely unexplored.

Amphiregulin (AREG), a member of the epidermal growth factor (EGF) family, is initially produced as a membrane-bound 252-amino acid precursor (pro-AREG) and subsequently cleaved by matrix metalloproteases to release its soluble form [11, 12]. AREG is frequently overexpressed in cancers and correlates with poor prognosis [13]. Beyond its well-characterized function as a ligand for the EGF receptor, AREG can translocate to the nucleus and influence transcriptional programs [14, 15]. Notably, AREG has been implicated in promoting apoptosis under DNA-damaging conditions: p53 induces its expression, and nuclear AREG regulates the processing of microRNAs such as miR-15a, ultimately repressing the anti-apoptotic protein Bcl-2 [16].

Here, we report a previously unrecognized mechanism linking mitochondrial Gln metabolism to DNA damage-induced cell death via AREG. We show that inhibiting Gln metabolism increases AREG transcription through the activation of the Max-like protein X (MLX) transcription factor. Importantly, mitochondrial Gln metabolism controls the sensitivity of cancer cells to chemotherapy, highlighting its potential as a metabolic vulnerability. Our findings provide new insights into how glutaminolysis influences cell fate after DNA damage and suggest potential therapeutic strategies targeting metabolic pathways in cancer.

## Materials and Methods

*Cell culture*

Mouse embryonic fibroblasts (MEFs) were either immortalized via SV40 large T antigen or transformed with E1A and Ras at passage 4. The study also employed previously characterized cell lines, including HCT116, HEK293T, and Helga [9, 17]. Cells were maintained in Dulbecco's Modified Eagle's Medium (DMEM; Welgene, Gyeongsan, Republic of Korea) supplemented with 10% fetal bovine serum (FBS; Gibco, NY, USA) and penicillin-streptomycin (Biowest, Nuaillé, France) was used to maintain all cell cultures. Mycoplasma contamination was routinely checked in every culture using a commercially available detection kit (Takara Bio Inc., Shinga, Japan).

*Plasmids and reagents*

Primary antibodies employed in this study included Bcl-2 (#CSB-PA000983, Cusabio Biotech, Wuhan, China), β-actin (#ABT264, Sigma, St. Louis, MO, USA), caspase-3 (#9664S, Cell Signaling), Lamin B1 (#12586S, Cell Signaling), MLX (#85570S, Cell Signaling Technology, Danvers, MA, USA), AREG (#sc74501, Santa Cruz Biotechnology, Dallas, TX, USA), GAPDH (#CSB-PA00025A0Rb, Cusabio Biotech, Wuhan, China), and GLS (#ab93434, Abcam, Cambridge, MA, USA).Small molecules and chemical reagents included aminooxyacetate (AOA), epigallocatechin gallate (EGCG), dimethyl-α-ketoglutarate (DMKG), N-acetylcysteine (NAC), glutathione, doxorubicin (DOX), cisplatin, camptothecin, etoposide (ETS), and 5-fluorouracil (Sigma). BPTES was sourced from CB-839 from Selleckchem (Houston, TX, USA) and Cayman Chemical (Ann Arbor, MI, USA). shRNA constructs targeting AREG (SHCLNDTRCN0000117996 and SHCLNDTRCN0000117992) were purchased from Sigma, whereas GLS-targeting shRNAs have been described previously [10].

*Western blotting*

Cells were lysed in EZ-RIPA buffer (ATTO, Tokyo, Japan) supplemented with protease and phosphatase inhibitors (ATTO). Lysates were cleared, and protein content was quantified before separation via SDS-polyacrylamide gel electrophoresis (SDS-PAGE). Following electrophoresis, proteins were transferred onto nitrocellulose membranes, which were blocked in Tris-buffered saline containing 5% bovine serum albumin and 0.1% Tween-20 (TBS-T) for 1 h. Membranes were incubated with primary antibodies overnight at 4 °C. After washes in TBS-T, membranes were incubated with horseradish peroxidase-conjugated secondary antibodies for 1 h at room temperature. Protein bands were detected using enhanced chemiluminescence (ECL; Promega, Madison, WI, USA) and imaged with a luminescent imaging system.

*Quantification and RNA extraction*

Total RNA was isolated from cells using RNAiso Plus (Takara Bio Inc., Shinga, Japan) following the manufacturer's instructions. For complementary DNA synthesis, 0.5 µg of RNA was reverse-transcribed with the iScript cDNA synthesis kit (Takara Bio Inc.). The resulting cDNA was diluted and subjected to quantitative PCR using SYBR Green I Mastermix on a LightCycler

480 system (Roche, South San Francisco, CA, USA). Target gene expression was normalized to β-actin. Primers were as follows: reverse 5′-CTTCCCAGAGTAGGTGTCATTG-3′ and human AREG, forward 5′-GCTGTCGCTCTTGATACTCG-3′; human β-actin, forward 5′-CTACGTCGCCCTGGACTTCGAGC-3′ and reverse 5′-GATGGAGCCGCCGATCCACACGG-3′; mouse Areg, forward 5′-CACCATAAGCGAAATGCCTTC-3′ and reverse 5′-TCTTGGGCTTAATCACCTGTTC-3′; mouse β-actin, forward 5′-AGCCATGTACGTAGCCATCC-3′ and reverse 5′-CTCTCAGCTGTGGTGGTGAA-3′. For assessing precursor miRNA levels, specifically pre-miR-15a, cDNA was generated using the ReverTra Ace™ qPCR RT kit (Toyobo, Osaka, Japan). Relative pre-miR-15a abundance was measured by RT-qPCR with reverse primer 5′-TCCTTGTATTTTGAGGC-3′ and forward primer 5′-CCCTTGGAGTAAAGTAG-3′, with GAPDH mRNA serving as a reference.

*SiRNA-mediated knockdown*

Cells were transfected with 25 nM siRNA immediately after plating at 30–50% confluency, depending on the experiment, using Lipofectamine RNAiMAX (Invitrogen, Carlsbad, CA, USA) according to the manufacturer's instructions. Cells were collected 24–36 h after transfection for downstream analyses as indicated in the figure legends. AREG-targeting siRNAs were purchased from Sigma (cat#: EMU025631).

*Assessment of cell death by flow cytometry*

For flow cytometric analysis, cells were treated with DNA-damaging agents before reaching 80% confluence. Post-treatment, cells were trypsinized, pelleted by centrifugation, and resuspended in PBS containing 3% FBS. Cell death was detected by propidium iodide (PI) staining, and quantification was performed using a flow cytometer as previously described.

*Assessment of cell viability*

For viability assays, cells were seeded at 1,000 cells per well in 100 µL of complete medium in 96-well plates. After 24 hours, the medium was replaced with fresh medium containing either doxorubicin (DOX) or etoposide (ETS). Three days later, cell viability was quantified using the CellTiter-Glo assay (Promega) following the manufacturer's instructions.

*Immunofluorescence staining*

Cells were fixed with 4% paraformaldehyde at room temperature for 5 minutes and permeabilized for 20 minutes with PBS containing 0.5% Triton X-100. Following two washes with PBS, cells were blocked in 5% normal goat serum (NGS) in 0.1% PBST for 1 hour. Cells were incubated overnight at 4 °C with an anti-AREG antibody (R&D Systems, Minneapolis, MN, USA) in 0.1% PBST containing 5% NGS. After three washes, FITC-conjugated streptavidin was applied for 1 hour at room temperature. Finally, cells were washed five times in 0.1% PBST and mounted with Vectashield containing DAPI (Vector Laboratories, Burlingame, CA, USA). Images were captured using confocal microscopy.

*Immunohistochemistry*

Tumor tissues were fixed in 4% paraformaldehyde, paraffin-embedded, and sectioned at 3 µm thickness. Sections were deparaffinized, rehydrated, and subjected to antigen retrieval in citrate buffer (95 °C, ImmunoBioScience, Mukilteo, WA, USA). Endogenous peroxidase activity was blocked with 1.4% hydrogen peroxide in methanol. Slides were blocked with 2.5% normal horse serum for 1 hour and incubated overnight at 4 °C with cleaved caspase-3 antibody (Cell Signaling). After three washes in PBS, sections were incubated with HRP-conjugated secondary antibody for 1 hour at room temperature. Signals were visualized using DAB (Vector Laboratories), and slides were counterstained with mounted with Permount (Fisher Scientific, Waltham, MA, USA) and Harris Hematoxylin (YD Diagnostics, Yongin, Korea), dehydrated in graded ethanol. Images were acquired with an Axio Scan.Z1 microscope (ZEISS, Oberkochen, Germany).

*In vivo experiments*

All animal procedures were conducted according to NIH guidelines and approved by the Catholic University of Korea College of Medicine Animal Ethics Committee. Male BALB/c nude mice (8 weeks old, n = 20) were obtained from Orient Bio (Seongnam, Korea) and randomly assigned to four groups (n = 5). Mice were injected subcutaneously in the abdominal flank with $1 \times 10^6$ transformed MEFs in a 1:1 mixture of PBS and Matrigel (50 µL each). Treatment groups included vehicle control, BPTES (12.5 mg/kg), ETS (20 mg/kg), and combination therapy (BPTES + ETS). Drugs were administered intraperitoneally six times at 24-hour

intervals when tumors reached ~100 $mm^3$. Tumors were harvested one day after the final treatment.

*Luciferase reporter assays*

The human AREG promoter was cloned into the pGL3 basic vector to generate a pGL3-AREG construct. Cells were co-transfected with pGL3-AREG and Renilla luciferase-expressing pRL-TK plasmid. After 18 hours, cells were treated with the indicated drugs for 24 hours. Luciferase activity was measured using the manufacturer's protocol (Promega), and firefly luciferase was normalized to Renilla luciferase. Mutations in the AREG promoter were introduced using the QuickChange site-directed mutagenesis kit (Agilent Technologies, CA, USA) with primers: 5′-GCGAATCCTTACGAAAAAGGGAGGCGGGGCG-3′ and 5′-CGCCCCGCCTCCCTTTTTCGTAAGGATTCGC-3′.

*Statistical analysis*

Unless otherwise indicated, data were analyzed using unpaired two-tailed Student's t-tests. Experiments were repeated independently at least two to three times, and each condition included at least three biological replicates ($n \geq 3$).

## Results and Discussion

*Mitochondrial glutamine metabolism modulates cellular response to DNA damage*

Given recent evidence that suppression of mitochondrial glutaminolysis is required for proper DNA damage responses, including cell cycle arrest and DNA repair [10], we investigated whether mitochondrial Gln metabolism influences cell survival following genotoxic stress. Glutaminase (GLS), the key enzyme driving mitochondrial glutaminolysis, controls the entry of Gln into mitochondria, and its inhibition effectively limits this metabolic pathway. Notably, we observed that treatment with the GLS inhibitor bis-2-(5-phenylacetoamido-1,2,4-thiadiazol-2-yl)ethyl sulfide (BPTES) [18] significantly decreased cell viability in the presence of the chemotherapeutic agent doxorubicin (DOX) [19], a widely used drug in cancer therapy **(Figure 1a)**. Conversely, enhancing mitochondrial glutaminolysis by administering dimethyl-α-ketoglutarate (DMKG) [20] conferred increased resistance to DOX-induced cytotoxicity **(Figure 1a).**

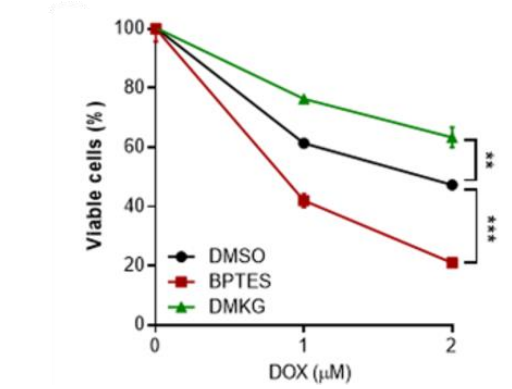


a)

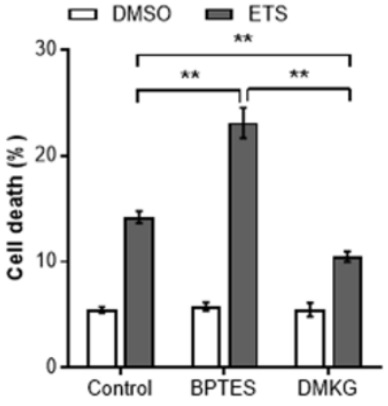


b)

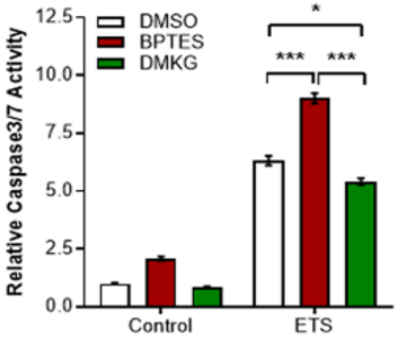


c)

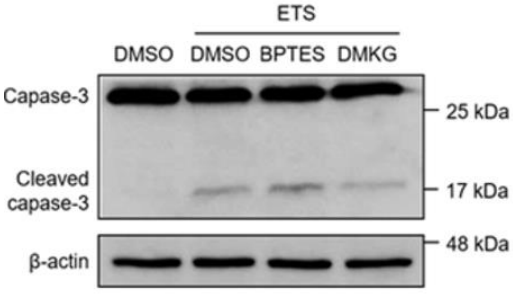


d)

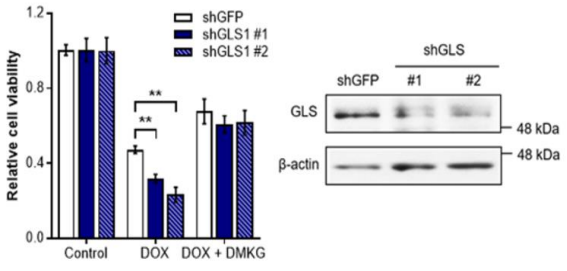


e)

**Figure 1.** Mitochondrial Glutamine Metabolism Modulates DNA Damage-Induced Apoptosis
a Cell viability of immortalized MEFs treated with DOX in combination with BPTES or DMKG (n = 3). Statistical significance was assessed using two-way ANOVA; data represent mean ± SD. b Survival of ETS-treated cells under BPTES or DMKG exposure (n = 3), measured by propidium iodide exclusion. c Caspase-3/7 activity in ETS-treated cells following GLS inhibition or DMKG supplementation (n = 4). d Immunoblot showing cleaved caspase-3 in ETS-treated cells; β-actin as loading control. e Relative viability of cells expressing control or GLS1-targeting shRNAs, with or without DMKG, following DOX exposure (n = 3), with GLS1 expression levels indicated (right). Error bars represent ± SEM. *p < 0.05, **p < 0.01, ***p < 0.001.

To examine whether mitochondrial glutamine metabolism directly influences apoptosis triggered by DNA damage, we treated cells with DOX or etoposide (ETS) [21]. Limiting Gln entry into the mitochondria through GLS inhibition significantly increased cell death, whereas boosting mitochondrial Gln flux with DMKG provided a protective effect **(Figure 1b)**. These changes in cell viability correlated with elevated caspase-3/7 activity and accumulation of cleaved caspase-3 protein **(Figures 1c and 1d)**. Similar results were obtained in GLS knockdown cells, confirming that mitochondrial Gln metabolism critically determines susceptibility to genotoxic stress-induced apoptosis **(Figure 1e)**. Together, these findings highlight mitochondrial glutaminolysis as a key metabolic checkpoint for cell survival following DNA damage.

*Mitochondrial glutamine metabolism governs AREG expression*

Since inhibiting Gln metabolism enhanced apoptosis after DNA damage, we explored whether this effect is mediated through amphiregulin (AREG), a known pro-apoptotic factor in genotoxic stress [16]. Removing Gln from the culture medium strongly elevated AREG mRNA in immortalized MEFs, whereas glucose deprivation did not trigger a comparable response **(Figure 2a).**

We then tested whether mitochondrial glutaminolysis directly controls AREG levels using multiple pharmacologic inhibitors, including BPTES, DON, and CB-839 [22]. All inhibitors consistently induced AREG expression **(Figure 2b)**. Remarkably, supplementation with DMKG reversed this induction, indicating that α-ketoglutarate production downstream of mitochondrial Gln metabolism suppresses AREG expression **(Figure 2b)**. Similarly, GLS knockdown increased AREG levels **(Figure 2c).**

To further investigate the role of mitochondrial Gln-derived α-ketoglutarate in regulating AREG, we targeted alternative metabolic routes using aminooxyacetate (AOA) or epigallocatechin gallate (EGCG), which inhibit transaminases and glutamate dehydrogenase, respectively. Both treatments led to robust AREG upregulation, demonstrating that mitochondrial Gln metabolism exerts tight control over AREG expression and thereby influences apoptotic responses to DNA damage.

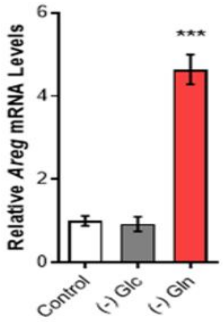


a)

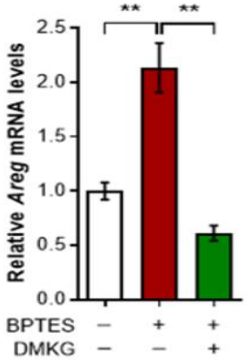


b)

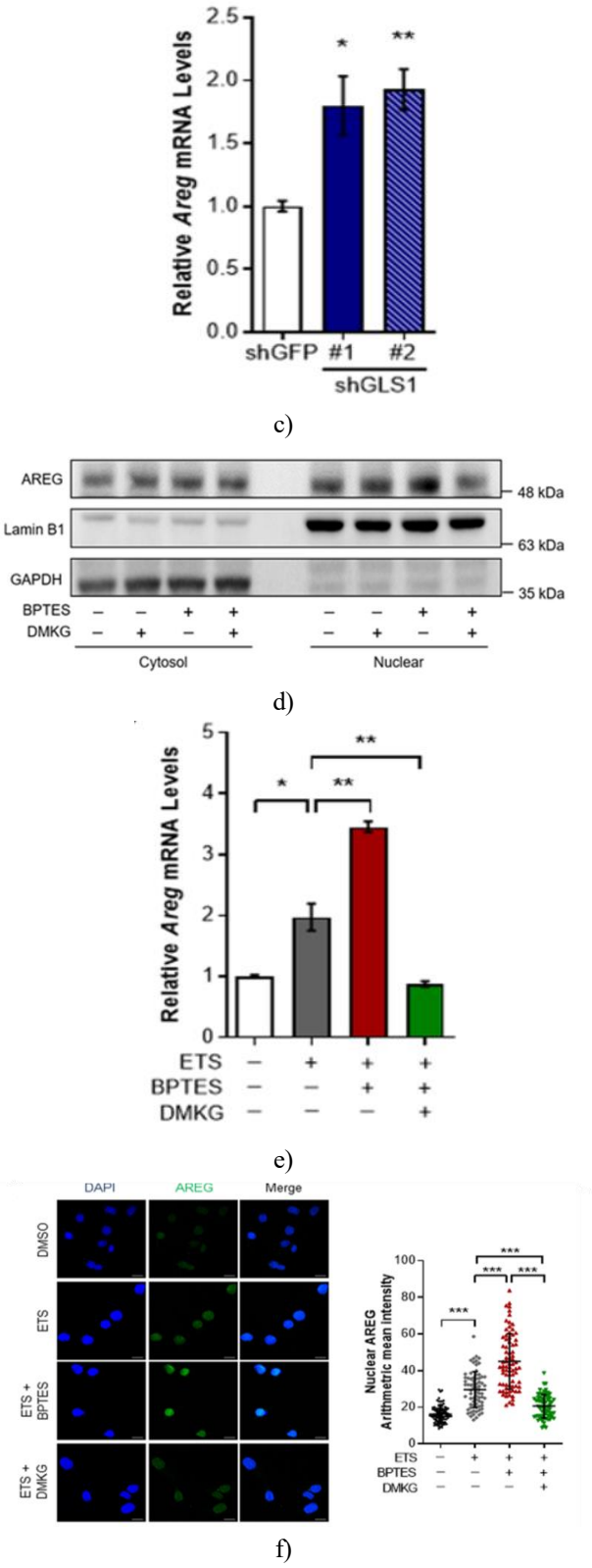


**Figure 2.** Mitochondrial glutamine metabolism influences AREG expression

a AREG mRNA levels were measured in immortalized MEFs cultured for 24 h with or without glutamine (Gln) or glucose (Glc) (n = 3). β-actin served as a qRT-PCR control. b Relative AREG expression after treatment with BPTES alone or combined with DMKG (n = 3). c AREG mRNA levels in HeLa cells expressing either control shRNA or two GLS-targeting shRNAs (n = 3). d Immunoblotting for AREG in cytoplasmic and nuclear fractions following BPTES, DMKG, or their combination; GAPDH and LaminB1 served as cytoplasmic and nuclear markers, respectively. e AREG mRNA in cells exposed to ETS alongside BPTES, DMKG, or both (n = 3). f Immunofluorescence of AREG (green) with nuclear DAPI staining under ETS treatment with BPTES or DMKG (DMSO: n = 100, ETS: n = 72, ETS + BPTES: n = 77, ETS + DMKG: n = 67). Scale bars: 2 µm. Nuclear mean AREG intensity is quantified on the right. Error bars indicate ± SEM. *p < 0.05, **p < 0.01, ***p < 0.001.

Because nuclear AREG contributes to apoptosis in response to DNA damage [16], we investigated whether blocking mitochondrial glutamine metabolism affects its nuclear accumulation. Subcellular fractionation revealed a robust increase in nuclear AREG following BPTES treatment, which was reversed when DMKG was supplied **(Figure 2d)**. To examine how Gln anaplerosis influences AREG induction during genotoxic stress, cells were treated with BPTES and/or DMKG prior to ETS exposure. ETS alone elevated AREG expression, as expected [16]; however, co-treatment with BPTES further amplified this response, while DMKG supplementation mitigated it **(Figure 2e).** Immunofluorescence analysis confirmed that these effects occurred predominantly in the nucleus **(Figure 2f).** These observations indicate that mitochondrial glutamine metabolism actively modulates both the levels and nuclear localization of AREG in response to DNA damage.

*AREG induction by mitochondrial glutamine metabolism is independent of p53*

To determine the transcriptional mechanisms controlling AREG under conditions of altered glutamine metabolism, we first assessed the role of p53, a known regulator of the AREG promoter [16]. Inhibition of p53 with pifithrin-α did not prevent AREG upregulation following GLS blockade **(Figure 3a).** Furthermore, BPTES treatment induced AREG in HEK293T cells with

inactive p53 and in p53-null PC3 prostate cancer cells **(Figure 3b)**. These results indicate that the mitochondrial glutamine-mediated regulation of AREG occurs independently of p53, suggesting the involvement of an alternative transcriptional regulator.

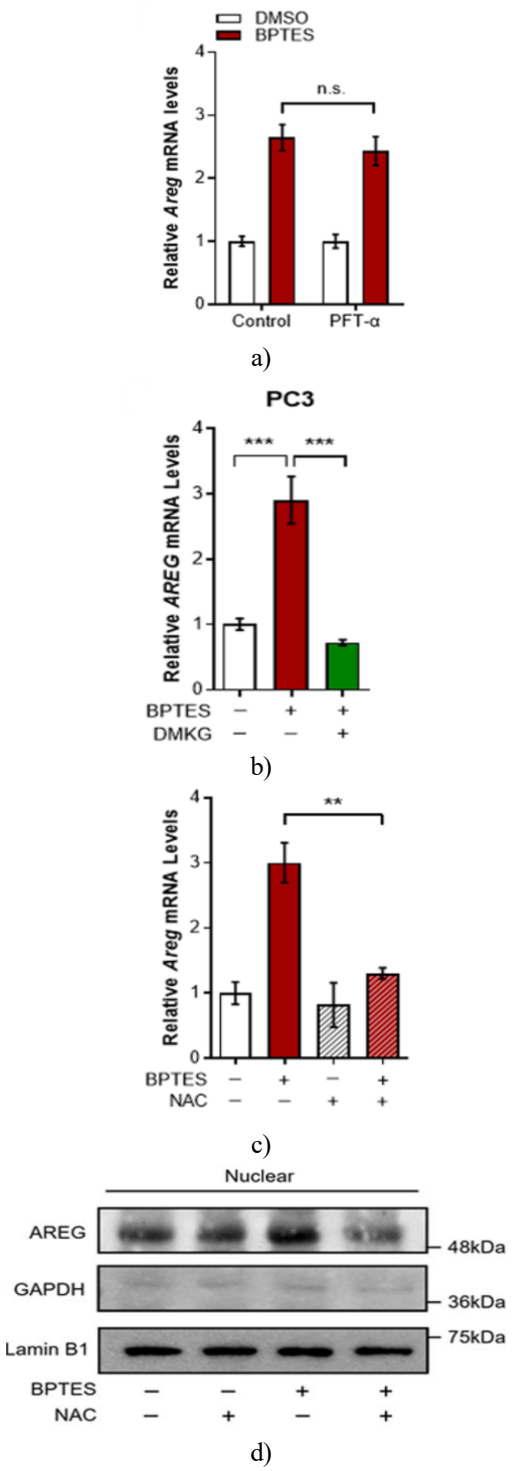


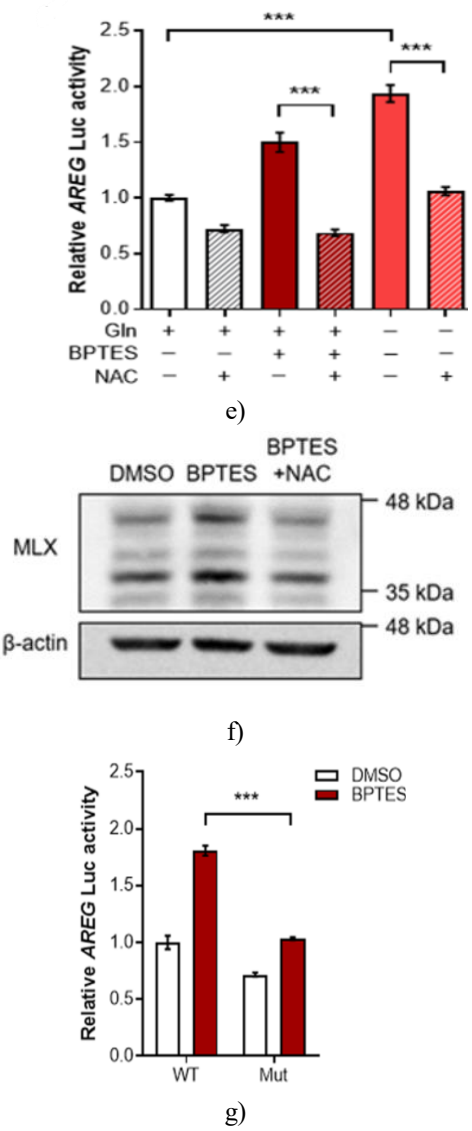


**Figure 3.** MLX Drives AREG Expression When Glutamine Anaplerosis Is Blocked

a AREG transcript levels in immortalized MEFs treated with various pharmacological agents (n = 3). b AREG mRNA in PC3 cells following exposure to BPTES, DMKG, or their combination (n = 3). c Changes in AREG mRNA in response to BPTES, the antioxidant NAC, or both (n = 3). d Nuclear accumulation of AREG protein after treatment with BPTES and/or NAC; LaminB1 used as nuclear control. e Luciferase reporter activity driven by the AREG promoter under BPTES, Gln supplementation, and/or NAC conditions (n = 3). f MLX protein levels under BPTES, NAC, or combined treatment. g Luciferase activity of wild-type versus MLX-binding site mutant AREG promoter following

BPTES exposure (n = 3). Error bars ± SEM; n.s., not significant. **p < 0.01, ***p < 0.001.

Glutamine metabolism is crucial for maintaining intracellular redox equilibrium, supporting glutathione synthesis and NADPH production via Gln-derived aspartate, both of which help control reactive oxygen species (ROS) levels [23]. Given this connection, we tested whether increased ROS caused by GLS inhibition could trigger AREG expression. Treating cells with hydrogen peroxide resulted in a dose-dependent increase in AREG transcripts, indicating that ROS alone can induce AREG. To determine whether this ROS surge mediates GLS inhibition effects, cells were treated with the antioxidant N-acetylcysteine (NAC). NAC markedly blunted the induction of AREG by BPTES at both the mRNA and nuclear protein levels **(Figure 3c)**, d). Similar suppression was observed using a cell-permeable glutathione analogue. Consistent with transcriptional regulation, luciferase assays revealed that BPTES or Gln deprivation enhanced AREG promoter activity, which was largely inhibited by NAC **(Figure 3e).**

To identify transcriptional regulators of AREG under glutamine-limited conditions, we analyzed the human AREG promoter using the TRANSFAC database (http://genexplain.com). Ten candidate transcription factors were predicted, among which Max-like protein X (MLX) is known to link metabolism and gene expression [24]. Notably, the human AREG promoter contains a sequence with strong similarity to the canonical MLX recognition motif, suggesting MLX could mediate AREG induction. Supporting this, BPTES treatment increased MLX protein levels, and NAC reversed this effect **(Figure 3f)**, indicating that ROS production drives MLX upregulation. Furthermore, mutating the MLX consensus-binding site in the AREG promoter significantly reduced BPTES-induced luciferase activity **(Figure 3g)**, demonstrating that MLX directly regulates AREG transcription when mitochondrial glutamine metabolism is inhibited.

*AREG Is required for gln-dependent control of DNA damage-induced apoptosis*

Finally, we investigated whether AREG is necessary for the pro-apoptotic effects of glutamine anaplerosis inhibition. AREG expression was silenced using siRNA, and cells were treated with ETS in the presence or absence of BPTES. In control cells, GLS inhibition enhanced DNA damage-induced apoptosis, whereas AREG knockdown abolished this effect **(Figure 4a)**. Consistently, cell viability assays showed that the reduction in survival caused by BPTES was rescued in AREG-depleted cells **(Figure 4b)**. These results indicate that AREG acts as a critical mediator connecting mitochondrial glutamine metabolism to the regulation of cell death under genotoxic stress.

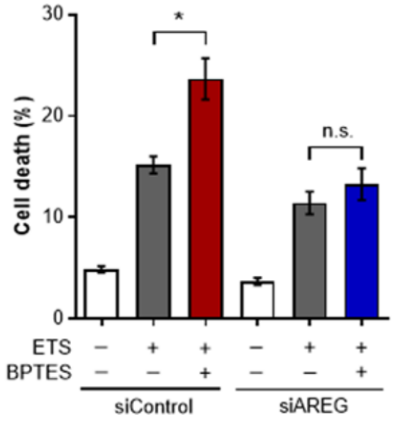


a)

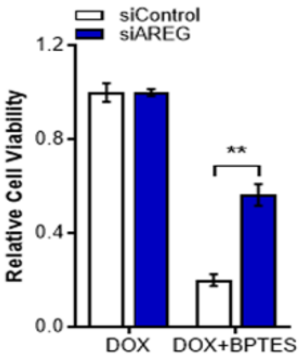


b)

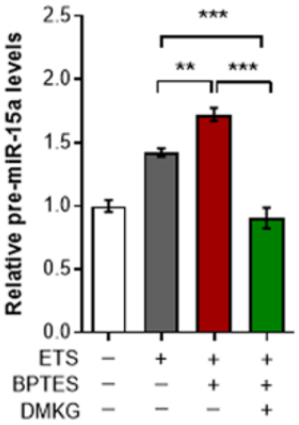


c)

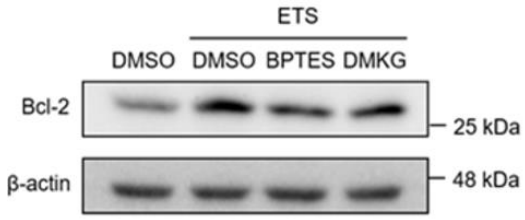


d)

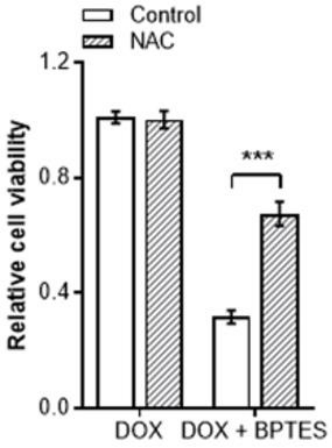


e)

**Figure 4.** AREG Links Mitochondrial Glutamine Metabolism to DNA Damage-Induced Apoptosis a Immortalized MEFs transfected with control siRNA (siControl) or siRNA targeting AREG (siAREG) were treated with ETS, BPTES, or both, and cell death was quantified (n = 3). b Cell viability of siControl and siAREG cells exposed to DOX, BPTES, or combined treatment (n = 3). c Precursor miR-15a levels were measured in cells treated with indicated compounds (n = 5). d Bcl-2 protein levels in ETS-treated cells under BPTES or DMKG conditions. e Viability of cells pre-treated with or without NAC, followed by DOX and/or BPTES exposure (n = 4). Error bars indicate ± SEM; n.s., not significant. *p < 0.05, **p < 0.01, ***p < 0.001.

Because AREG promotes apoptosis by enhancing processing of miR-15a, which in turn represses the anti-apoptotic protein Bcl-2 [16], we evaluated whether mitochondrial Gln metabolism affects this pathway. Cells with inhibited Gln anaplerosis displayed a stronger induction of pre-miR-15a following DNA damage, an effect that was attenuated by supplementation with DMKG **(Figure 4c).** Correspondingly, Bcl-2 protein levels decreased after BPTES treatment, and DMKG restored them to near-baseline levels **(Figure 4d**).

We then investigated whether ROS, elevated by GLS inhibition, contribute to the reduction in cell viability. Treating cells with NAC partially rescued cell survival under DNA damage conditions in the presence of BPTES, paralleling the suppression of AREG expression **(Figure 4e)**. These results collectively indicate that mitochondrial glutamine metabolism regulates DNA damage-induced apoptosis through a ROS-AREG-miR-15a-Bcl-2 axis.

*Targeting mitochondrial glutamine metabolism enhances chemotherapy sensitivity*

Chemotherapeutic agents predominantly eliminate cancer cells via DNA damage, yet intrinsic resistance remains a major barrier to efficacy [25, 26]. Our data suggest that limiting mitochondrial Gln metabolism can sensitize cells to DNA damage. In HeLa and HCT116 cancer cells, GLS inhibition or Gln deprivation strongly induced AREG, an effect reversed by DMKG **(Figure 5a)**. Importantly, pharmacological suppression of Gln anaplerosis using BPTES enhanced the cytotoxicity of DOX, resulting in elevated apoptosis and reduced cell **viability (Figures 5b and 5c)**. These findings demonstrate that mitochondrial glutamine metabolism is a key determinant of chemotherapeutic response and that targeting Gln anaplerosis may represent a viable strategy to potentiate DNA-damage-based cancer therapies.

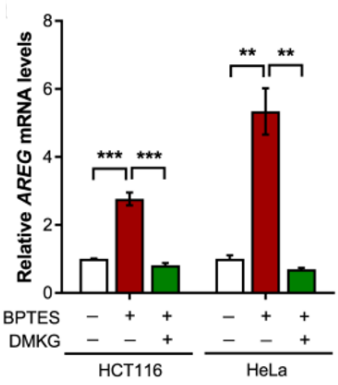


a)

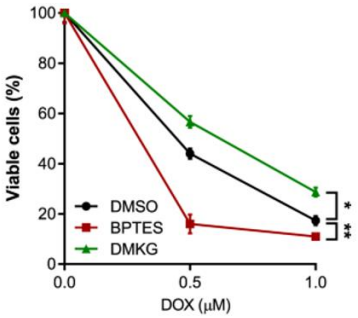


b)

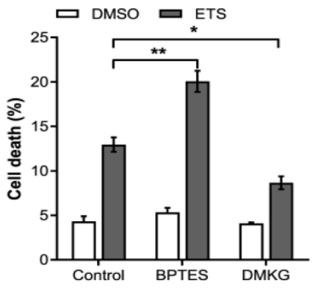


c)

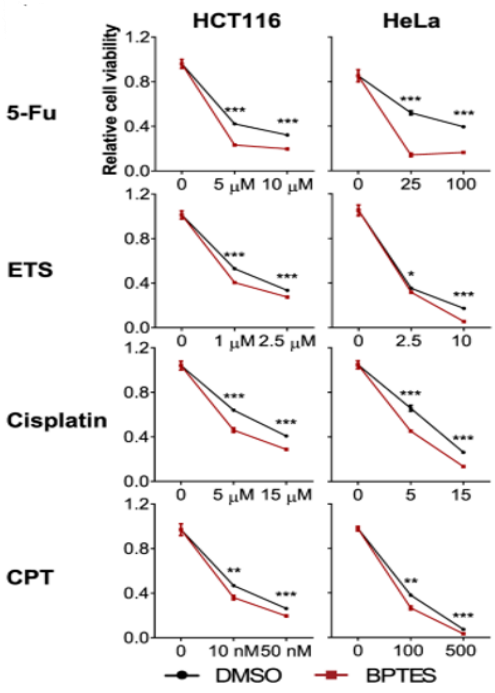


d)

**Figure 5.** Targeting Glutamine Anaplerosis Enhances Chemotherapy Sensitivity in Cancer Cells
a Levels of AREG mRNA in HCT116 and HeLa cells under different treatment conditions (n = 3). b Viability of HeLa cells exposed to DOX combined with either BPTES or DMKG (n = 3); statistical significance determined by two-way ANOVA. c Quantification of HeLa cell death following ETS treatment in the presence of BPTES or DMKG (n = 3). d Viability of HCT116 and HeLa cells treated with various DNA-damaging chemotherapeutic agents in combination with either DMSO or BPTES (n = 3). All error bars represent ± SEM. *p < 0.05, **p < 0.01, ***p < 0.001.

To assess whether mitochondrial glutamine metabolism influences cancer cell response to a broader range of chemotherapeutics, HCT116 and HeLa cells were co-treated with BPTES during drug exposure. Across multiple chemotherapeutic agents, cells receiving BPTES in combination exhibited substantially greater cell death compared to treatment with chemotherapy alone, revealing a synergistic effect **(Figure 5d).** These results indicate that inhibiting glutamine anaplerosis can potentiate the cytotoxicity of DNA-damaging drugs in cancer cells.

*GLS inhibition potentiates chemotherapy-induced apoptosis in vivo*

To determine whether these effects translate to tumors in vivo, allografts were generated using E1A/Ras-transformed MEFs. Once tumors reached approximately 100 mm³, mice were treated with ETS, BPTES, or the combination **(Figure 6a)**. Single-agent doses were selected to minimally impact tumor growth, allowing assessment of additive or synergistic effects. Tumors from mice receiving both BPTES and ETS exhibited a marked increase in AREG mRNA compared to ETS alone **(Figure 6b)**. Similarly, immunoblot analysis confirmed higher nuclear and total AREG protein levels in the combination-treated tumors **(Figure 6c)**, consistent with the in vitro findings. These results demonstrate that inhibition of mitochondrial glutamine metabolism can sensitize tumors to DNA-damaging chemotherapy by enhancing AREG-mediated apoptotic signaling, supporting a potential therapeutic strategy for improving chemotherapeutic efficacy.

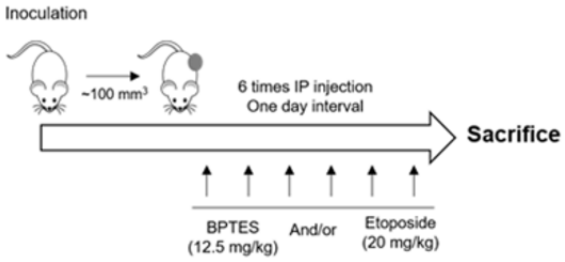


a)

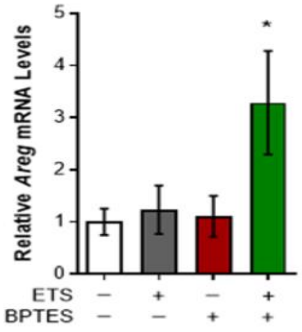


b)

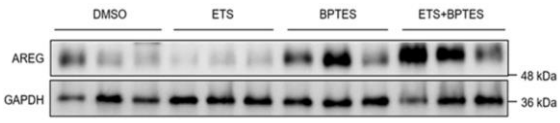


c)

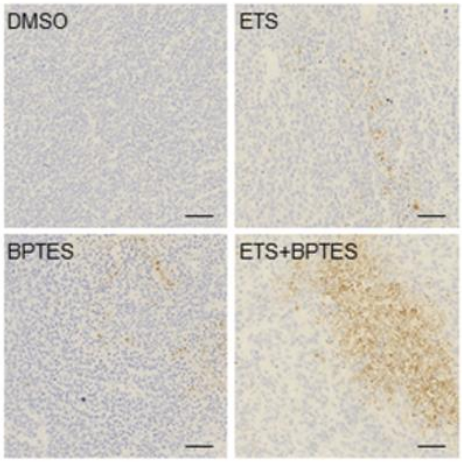


d)

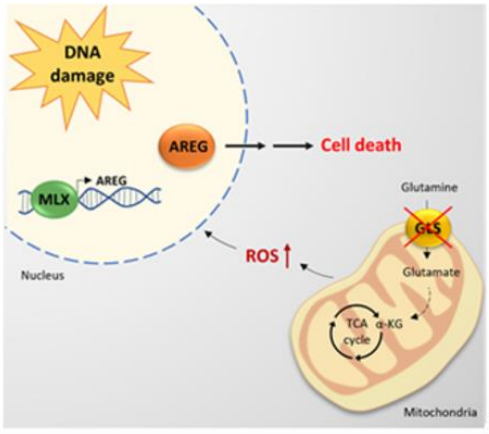


e)

**Figure 6.** GLS inhibition enhances chemotherapy-induced tumor cell death

a Schematic of the in vivo experimental design. Mice were subcutaneously injected with transformed MEFs, and treated with ETS, BPTES, or the combination. Tumors were harvested one day after treatment. b, c AREG expression in tumor tissues, assessed at the mRNA (b) and protein (c) levels following the indicated treatments (n = 3). d Immunohistochemistry for cleaved caspase-3 in allograft tumors; scale bars, 50 µm. e Proposed model depicting how mitochondrial glutamine metabolism modulates DNA damage-induced apoptosis. Error bars indicate ± SEM. *p < 0.05.

To evaluate whether mitochondrial glutamine metabolism affects tumor susceptibility to chemotherapy, we analyzed apoptosis in tumor tissues by immunohistochemistry. Treatment with either ETS or BPTES alone led to only modest increases in cleaved caspase-3, whereas the combination markedly elevated the number of apoptotic cells **(Figure 6d)**. These observations demonstrate that GLS inhibition sensitizes tumors to DNA-damaging chemotherapy in vivo.

*Proposed mechanistic model*

Collectively, our findings support a model in which mitochondrial glutamine metabolism regulates cellular responses to DNA damage through AREG. Inhibition of glutamine anaplerosis increases ROS, which activates MLX-dependent transcription of AREG. Nuclear AREG then promotes miR-15a processing, leading to suppression of anti-apoptotic proteins such as Bcl-2, ultimately enhancing caspase-dependent apoptosis. By targeting this metabolic pathway, chemotherapeutic efficacy can be potentiated both in vitro and in vivo **(Figure 6e).** This mechanism highlights mitochondrial glutaminolysis as a promising therapeutic target to improve outcomes in DNA-damage-based cancer treatments.

In this work, we reveal that mitochondrial glutamine (Gln) metabolism plays a key role in modulating DNA damage-induced apoptosis via amphiregulin (AREG) **(Figure 6e).** Previous studies have established that AREG is essential for executing apoptosis in response to genotoxic stress [16]. Here, we extend these findings by demonstrating that GLS inhibition elevates reactive oxygen species (ROS), which further stimulates AREG transcription following DNA damage. Notably, silencing AREG attenuates the enhanced apoptosis induced by GLS inhibition, highlighting its critical role in linking glutamine metabolism to cell death. This concept is reinforced by our observation that modulating Gln anaplerosis influences cancer cell sensitivity to chemotherapeutic agents, emphasizing the therapeutic relevance of this pathway. Collectively, these findings uncover a previously unappreciated function of mitochondrial Gln metabolism in directing the cell fate decision between survival and apoptosis under DNA damage, with significant implications for cancer therapy. Our results align with prior work demonstrating that repression of mitochondrial Gln metabolism is required for an effective DNA damage response [10]. For instance, Jeong *et al*. (2013) showed that genotoxic stress

blocks Gln entry into the TCA cycle, a step necessary for proper cell cycle arrest and DNA repair, and that failure of this block promotes genomic instability and tumorigenesis. In agreement with this, pharmacological disruption of Gln anaplerosis in our study led to a marked increase in cell death following DNA damage. Considering that inefficient clearance of DNA-damaged cells can facilitate chromosomal instability and tumor development, both our work and that of Jeong *et al*. highlight mitochondrial Gln metabolism as a key metabolic checkpoint for maintaining genomic stability and preventing cancer progression.

Although our data emphasize the role of AREG in mediating the pro-apoptotic effects of Gln anaplerosis inhibition, other Gln-dependent pathways may also contribute to cell survival under genotoxic stress. Gln is a major contributor to redox homeostasis by supporting glutathione synthesis [27], an essential antioxidant that protects against oxidative DNA damage. Additionally, Gln provides substrates for nucleotide biosynthesis and NADPH production [22], both critical for DNA repair. In some tissues, liver-type cells express GLS2 [28], which is induced by DNA damage via a p53-dependent mechanism [29]. Future studies will be necessary to elucidate whether these and other branches of Gln metabolism influence cell fate decisions after DNA damage.

Cancer cells display distinct metabolic adaptations, including enhanced glycolysis and reduced oxidative phosphorylation [30], often accompanied by hypoxia and elevated HIF1α levels. HIF1α inhibits pyruvate dehydrogenase (PDH), limiting conversion of pyruvate to acetyl-CoA; under these conditions, Gln becomes essential to replenish the TCA cycle [8]. Moreover, GLS inhibition can further activate HIF1α by reducing α-ketoglutarate (αKG), potentially exacerbating PDH inhibition. Consequently, Gln anaplerosis suppression may lower TCA intermediates and sensitize cancer cells to DNA damage. This notion is supported by observations that NAC can restore TCA intermediates by enhancing carbon flux through pyruvate decarboxylase [31]. Additionally, some cancer cells can bypass GLS inhibition by activating alternative metabolic pathways [32, 17], suggesting that adaptive metabolic responses may contribute to resistance against DNA-damaging therapies.

While our study focuses on exploiting Gln anaplerosis inhibition to enhance chemotherapy-induced cancer cell death, it is important to acknowledge the beneficial roles of Gln metabolism in normal tissues. For example, intestinal epithelium and immune cells rely on Gln for energy, particularly to recover from genotoxic stress induced by chemotherapy or radiation [30]. Furthermore, Gln consumption is necessary to replenish glutathione and support tissue regeneration after DNA damage [30]. Therefore, additional research will be needed to delineate the differential roles of Gln metabolism in cancer versus normal tissues during treatment.

These findings provide a rationale for potential therapeutic strategies targeting glutamine metabolism. DNA-damaging agents, including chemotherapy and radiotherapy, remain mainstays of cancer treatment [3, 33], yet resistance frequently arises due to enhanced DNA repair or anti-apoptotic signaling [25, 34]. Our results demonstrate that GLS inhibition promotes AREG-mediated apoptosis, thereby sensitizing cancer cells to genotoxic therapies. Considering that many tumors are glutamine-addicted [8, 35] and that clinical-grade GLS inhibitors are under development [36], these data have significant translational potential for improving the efficacy of DNA-damage-based cancer therapies.

## Conclusion

In conclusion, we identify a direct mechanistic link between mitochondrial Gln metabolism and DNA damage-induced apoptosis through AREG. Our work underscores the critical role of metabolic stress responses in regulating cell fate under genotoxic conditions and highlights mitochondrial Gln metabolism as a promising therapeutic target in cancer treatment.

**Acknowledgments:** This research was supported by the National Research Foundation of Korea (NRF) grant funded by the Korea government (2019R1A2C1089937 and 2019R1I1A1A01059928).

**Conflict of Interest:** None

**Financial Support:** None

**Ethics Statement:** None

## References

1. Ciccia A, Elledge SJ. The DNA damage response: making it safe to play with knives. Mol. Cell. 2010;40:179–204.

2. Turgeon MO, Perry NJS, Poulogiannis G. DNA damage, repair, and cancer metabolism. Front Oncol. 2018;8:15.
3. Lord CJ, Ashworth A. The DNA damage response and cancer therapy. Nature. 2012;481:287–94.
4. Zhu JJ, Thompson CB. Metabolic regulation of cell growth and proliferation. Nat. Rev. Mol. Cell Bio. 2019;20:436–50.
5. Jones RG, Thompson CB. Tumor suppressors and cell metabolism: a recipe for cancer growth. Genes Dev. 2009;23:537–48.
6. Altman BJ, Stine ZE, Dang CV. From Krebs to clinic: glutamine metabolism to cancer therapy. Nat. Rev. Cancer. 2016;16:749.
7. Cluntun AA, Lukey MJ, Cerione RA, Locasale JW. Glutamine metabolism in cancer: understanding the heterogeneity. Trends Cancer. 2017;3:169–80.
8. Wise DR, Thompson CB. Glutamine addiction: a new therapeutic target in cancer. Trends Biochem Sci. 2010;35:427–33.
9. Yang S, Hwang S, Kim M, Seo SB, Lee JH, Jeong SM. Mitochondrial glutamine metabolism via GOT2 supports pancreatic cancer growth through senescence inhibition. Cell Death Dis. 2018;9:55.
10. Jeong SM, Xiao C, Finley LW, Lahusen T, Souza AL, Pierce K, et al. SIRT4 has tumor-suppressive activity and regulates the cellular metabolic response to DNA damage by inhibiting mitochondrial glutamine metabolism. Cancer Cell. 2013;23:450–63.
11. Brown CL, Meise KS, Plowman GD, Coffey RJ, Dempsey PJ. Cell surface ectodomain cleavage of human amphiregulin precursor is sensitive to a metalloprotease inhibitor. Release of a predominant N-glycosylated 43-kDa soluble form. J. Biol. Chem. 1998;273:17258–68.
12. Berasain C, Avila MA. Amphiregulin. Semin Cell Dev. Biol. 2014;28:31–41.
13. Busser B, Sancey L, Brambilla E, Coll JL, Hurbin A. The multiple roles of amphiregulin in human cancer. Biochim Biophys. Acta. 2011;1816:119–31.
14. Isokane M, Hieda M, Hirakawa S, Shudou M, Nakashiro K, Hashimoto K, et al. Plasma-membrane-anchored growth factor pro-amphiregulin binds A-type lamin and regulates global transcription. J. Cell Sci. 2008;121:3608–18.
15. Johnson GR, Saeki T, Auersperg N, Gordon AW, Shoyab M, Salomon DS, et al. Response to and expression of amphiregulin by ovarian carcinoma and normal ovarian surface epithelial cells: nuclear localization of endogenous amphiregulin. Biochem Biophys. Res Commun. 1991;180:481–8.
16. Taira N, Yamaguchi T, Kimura J, Lu ZG, Fukuda S, Higashiyama S, et al. Induction of amphiregulin by p53 promotes apoptosis via control of microRNA biogenesis in response to DNA damage. Proc. Natl Acad. Sci. USA. 2014;111:717–22.
17. Kim M, Gwak J, Hwang S, Yang S, Jeong SM. Mitochondrial GPT2 plays a pivotal role in metabolic adaptation to the perturbation of mitochondrial glutamine metabolism. Oncogene. 2019;38:4729–38.
18. Robinson MM, McBryant SJ, Tsukamoto T, Rojas C, Ferraris DV, Hamilton SK, et al. Novel mechanism of inhibition of rat kidney-type glutaminase by bis-2-(5-phenylacetamido-1,2,4-thiadiazol-2-yl)ethyl sulfide (BPTES). Biochem J. 2007;406:407–14.
19. Yang F, Teves SS, Kemp CJ, Henikoff S. Doxorubicin, DNA torsion, and chromatin dynamics. Biochim Biophys. Acta. 2014;1845:84–89.
20. Jeong SM, Hwang S, Seong RH. SIRT4 regulates cancer cell survival and growth after stress. Biochem Biophys. Res Commun. 2016;470:251–6.
21. Montecucco A, Zanetta F, Biamonti G. Molecular mechanisms of etoposide. EXCLI J. 2015;14:95–108.
22. Gross MI, Demo SD, Dennison JB, Chen L, Chernov-Rogan T, Goyal B, et al. Antitumor activity of the glutaminase inhibitor CB-839 in triple-negative breast cancer. Mol. Cancer Ther. 2014;13:890–901.
23. Yoo HC, Yu YC, Sung Y, Han JM. Glutamine reliance in cell metabolism. Exp. Mol. Med. 2020;52:1496–516.
24. Havula E, Hietakangas V. Glucose sensing by ChREBP/MondoA-Mlx transcription factors. Semin Cell Dev Biol. 2012;23:640–7.
25. Schirrmacher V. From chemotherapy to biological therapy: a review of novel concepts to reduce the side effects of systemic cancer treatment (Review). Int J Oncol. 2019;54:407–19.
26. Mansoori B, Mohammadi A, Davudian S, Shirjang S, Baradaran B. The different mechanisms of cancer drug resistance: a brief review. Adv Pharm Bull. 2017;7:339–48.

27. Alberghina L, Gaglio D. Redox control of glutamine utilization in cancer. Cell Death Dis. 2014;5:e1561.
28. Curthoys NP, Watford M. Regulation of glutaminase activity and glutamine metabolism. Annu Rev Nutr. 1995;15:133–59.
29. Suzuki S, Tanaka T, Poyurovsky MV, Nagano H, Mayama T, Ohkubo S, et al. Phosphate-activated glutaminase (GLS2), a p53-inducible regulator of glutamine metabolism and reactive oxygen species. Proc. Natl Acad. Sci. USA. 2010;107:7461–6.
30. Michalak KP, Mackowska-Kedziora A, Sobolewski B, Wozniak P. Key roles of glutamine pathways in reprogramming the cancer metabolism. Oxid Med Cell Longev. 2015;2015:964321.
31. Zwingmann C, Bilodeau M. Metabolic insights into the hepatoprotective role of N-acetylcysteine in mouse liver. Hepatology. 2006;43:454–63.
32. Biancur DE, Paulo JA, Malachowska B, Quiles Del Rey M, Sousa CM, Wang X, et al. Compensatory metabolic networks in pancreatic cancers upon perturbation of glutamine metabolism. Nat Commun. 2017;8:15965.
33. Hosoya N, Miyagawa K. Targeting DNA damage response in cancer therapy. Cancer Sci. 2014;105:370–88.
34. Vasan N, Baselga J, Hyman DM. A view on drug resistance in cancer. Nature. 2019;575:299–309.
35. Zhang J, Pavlova NN, Thompson CB. Cancer cell metabolism: the essential role of the nonessential amino acid, glutamine. EMBO J. 2017;36:1302–15.
36. Song M, Kim SH, Im CY, Hwang HJ. Recent development of small molecule glutaminase inhibitors. Curr Top Med Chem. 2018;18:432–43.